

# Soft Matter

Accepted Manuscript



This is an *Accepted Manuscript*, which has been through the Royal Society of Chemistry peer review process and has been accepted for publication.

*Accepted Manuscripts* are published online shortly after acceptance, before technical editing, formatting and proof reading. Using this free service, authors can make their results available to the community, in citable form, before we publish the edited article. We will replace this *Accepted Manuscript* with the edited and formatted *Advance Article* as soon as it is available.

You can find more information about *Accepted Manuscripts* in the [Information for Authors](#).

Please note that technical editing may introduce minor changes to the text and/or graphics, which may alter content. The journal's standard [Terms & Conditions](#) and the [Ethical guidelines](#) still apply. In no event shall the Royal Society of Chemistry be held responsible for any errors or omissions in this *Accepted Manuscript* or any consequences arising from the use of any information it contains.

Cite this: DOI: 10.1039/c0xx00000x

www.rsc.org/xxxxxx

ARTICLE TYPE

# Mechano-responsive gelation of water precedes its thermo-gelation by a short alanine derivative

Amarendar Reddy M<sup>a</sup> and Aasheesh Srivastava<sup>a\*</sup>*Received (in XXX, XXX) Xth XXXXXXXXXX 20XX, Accepted Xth XXXXXXXXXX 20XX*

DOI: 10.1039/b000000x

We report design of a structurally-concise alanine derivative (**Ala-hyd**) that has a rotationally flexible aromatic *N*-protecting group for alanine, and a hydrazide functionality at its carboxylic end. **Ala-hyd** requires mechanical agitation (physical shaking, vortexing or sonicating) to form supramolecular hydrogels at medium concentrations (0.4–0.8 wt%). At higher concentrations (>0.8 wt%), it gels water spontaneously upon undisturbed cooling of the hot solution, while at lower concentrations (<0.4 wt%), only turbid suspensions were formed upon agitation. In the <0.8 wt% regime, hydrogelation by **Ala-hyd** is modulated by its concentration as well as by the extent of mechanical agitation applied. Turbimetry and fluorescence spectroscopy indicate enhanced self-assembly of **Ala-hyd** upon agitation. FTIR studies point towards stronger hydrogen bonds in the resulting assemblies. Since **Ala-hyd** requires mechanical agitation to undergo self-assembly, its aqueous sols exhibited mild shear-thickening behaviour in buffered as well as salt-free conditions. During shearing, the formation of an entangled mesh of long, helical nanofibers coincided with the maximum in the bulk shear viscosity. pH-dependent rheological investigations indicate that protonation of the amine unit ( $pK_a = 8.9$ ) of hydrazide diminishes the self-assembly propensity of this compound. The self-assembly of **Ala-hyd** can thus be modulated through mechanical as well as chemical cues.

## 1 Introduction

Low molecular weight hydrogelators (LMHGs) are fascinating soft materials having direct utility in biomedical and drug-delivery applications.<sup>1,2,3,4</sup> Hydrogels derived from nanofibrillar self-assembly of small peptides are coveted due to their biocompatibility and low cytotoxicity.<sup>5,6,7</sup> An additional impetus to create supramolecular hydrogels from small peptides originates from our ability to control the inherent intermolecular interactions through chemical or physical means. Such stimuli-responsive supramolecular architectures can be utilized for controlled delivery of entrapped drug, or for sensing anions.<sup>8,9</sup> Hydrogen bonding,  $\pi$ - $\pi$  stacking, van der Waals' and hydrophobic interactions are routinely involved in the self-assembly of LMHGs.<sup>10,11,12</sup> Recently, halogen-bonding interactions have also been exploited for supramolecular self-assembly.<sup>13,14,15</sup>

While researchers have created numerous chemo-responsive self-assembling systems,<sup>16,17,18</sup> mechano-responsive self-assembly has received scientific attention only recently. Generally mechanical agitation disrupts the non-covalent interactions between small molecules, resulting in the physical disruption of gel. This thixotropic behaviour is common for gels prepared from low molecular weight gelators, and has been reported for a very wide variety of systems.<sup>19,20,21,22</sup> The inverse phenomenon, whereupon mechanical agitation causes an increase in solution viscosity is typically exhibited by polymers such as corn starch, and is attributed to the entanglement of macromolecular chains.<sup>23,24,25</sup> Nevertheless, a few low molecular-

weight systems have been reported to self-assemble under mechanical agitation, such as the cyclic dipeptide reported by Feng's group.<sup>26</sup> Similarly, Tirelli and co-workers studied the effect of mechanical agitation on the properties and the nanoscale morphologies of assemblies being formed by aromatic peptides Fmoc-FF and Fmoc-GG.<sup>27</sup> The self-association of carbazole-based bisureas in organic solvents by mechanical agitation was also recently reported by Feringa's group.<sup>28</sup> Such agitation-induced self-assembly is thought to happen due to the introduction of nucleation in the metastable supersaturated solutions of these compounds due to mechanical agitation.

In this work, we report the design, synthesis, and hydrogelation ability of a short alanine derivative (**Ala-hyd**) in biologically relevant conditions (i.e. in buffered as well as salt-free aqueous medium). While at concentrations >0.8 wt%, **Ala-hyd** acted as a thermogelator, at concentrations below this, it required mechanical agitation to undergo self-assembly, and to form hydrogels in 0.4–0.8 wt% regime. In the following sections, we describe our investigations into the agitation-induced self-assembly of **Ala-hyd** through a variety of techniques such as fluorescence and UV-vis spectroscopy, FTIR, as well as rheological studies, and AFM and SEM microscopy.

## 2 Experimental Section

### 2.1 Materials and methods

1-Naphthylacetic acid (1-NAA) and hydrazine hydrate were purchased from Spectrochem, 1,1-Carbonyl diimidazole (CDI)

was purchased from Alfa Aesar. Sodium hydroxide, Hydrochloric acid, Triethylamine were obtained from Merck. Sodium sulphate was obtained from Rankem. All solvents used in the synthesis were dried, or distilled, as required. Details of synthesis and characterization of **Ala-hyd** are provided in the ESI, Scheme S1. NMR spectra ( $^1\text{H}$  and  $^{13}\text{C}$ ) recorded on a Bruker Ultra shield (400MHz) spectrometer are shown in Fig. S4 and S5, ESI.

## 2.2 Self-assembly

5 mg of **Ala-hyd** was suspended in 1 mL of distilled water in glass vial. The suspension was heated at 80 °C for 5 min to obtain clear solution, which was kept undisturbed at room temperature. No turbidity was observed visually even two days after the solution attained room temperature. However, if the same solution was agitated mechanically (either by vortexing, stirring or hand shaking), an opaque gel could be obtained. Above 8 mg/mL concentration, gel was formed spontaneously upon undisturbed cooling of the solution for *ca.* 30 min. The assembly of **Ala-hyd** was not influenced by the presence of salts, and similar results were obtained on using 50 mM phosphate buffer (PB) to maintain the pH.

## 2.3 Turbimetry

**Ala-hyd** was dissolved in buffered aqueous solution (50 mM PB, pH = 7) at 1 mg/mL concentration and the turbidity changes in the solutions were measured for samples that were either vortexed for a certain duration of time at 2000 rpm, or were left un-agitated. Absorbance at 600 nm were monitored for these samples after 1, 2, 3, 4, 5, and 6 min.

## 2.4 FTIR Spectroscopy

Both vortexed and non-vortexed samples of **Ala-hyd** prepared in salt-free deuterium oxide were dried in vacuum desiccator for 24 h. FTIR spectra were recorded as KBr pellets on a PerkinElmer Spectrum BX FTIR spectrometer.

## 2.5 Fluorescence experiments

0.45 mg/mL **Ala-hyd** solution in 50 mM PB, pH=7 was used for the fluorescence studies. Fluorescence spectra were recorded on a Horiba Jobin Yvon Fluorolog 3-111 instrument. Spectra were recorded for samples before vortexing, and after vortexing at 2000 rpm for required duration (1-6 min) in a 10 mm path length quartz cuvette. The emission and the excitation slit widths were 2 nm. The samples were excited at 280 nm, and the resulting emission was recorded in the wavelength range of 300-500 nm.

## 2.6 Rheological studies

Time-dependent and time-independent experiments were performed at 25 °C on a Rheoplus MCR302 (Anton paar) rotational rheometer by using concentric cylinder bob-in-cup configuration (CC27). All the samples were prepared in 50 mM PB (pH=7). In time-dependent experiment viscosity was recorded against time at different shear rates (such as 2500 rpm, and 1500 rpm) and different concentrations. pH-dependent viscosity changes were also measured at pH=7 and 5 in 50 mM PB at 2500 rpm. For the oscillatory shear measurements, parallel top plate with a 25 mm diameter and 1.0 mm gap distance were used. Gels (7 mg/ml) for rheological experiments were scooped onto the

bottom plate of rheometer. The shear moduli (storage modulus  $G'$  and loss modulus  $G''$ ) were measured against % strain ( $\gamma$ ) from 0.1% to 100 %. Frequency sweep experiment was performed from 0.1 to 100 rad/s at constant strain of 1%.

## 2.7 Microscopy

For SEM, the samples were scraped from the surface of the bob of the rheometer at three different time points *viz.* 100 s, 800 s, and 1000 s. The extracted samples were dried inside vacuum desiccator for 48 h. These samples were spread on carbon tape and gold coated for 120 s. The images were recorded on Carl Zeiss (Ultraplus) FE-SEM used at 5 kV accelerating voltage. For AFM, samples were extracted from the surface of the bob of the rheometer at different time points (like 800 s and 1000 s), and dropped on freshly-cleaved mica surface. Samples were air dried for 1 h before AFM imaging. The images were obtained by scanning the mica surface in non-contact mode using NSC 19/AIBN cantilever (Micromash), length=125±5 nm, width=35±3 nm, thickness =1.0±0.5 nm, tip radius <10 nm, resonant frequency=80 kHz, force constant=0.6 Nm<sup>-1</sup>. AFM scans were recorded at 256 x 256 pixels resolution and topographic, amplitude and phase images were taken.

## 3 Results and Discussion

### 3.1 Design of hydrogelator

We have previously reported a series of amino acid based sono- and thermo-gelators having rotationally-flexible aromatic *N*-protecting group(s).<sup>10,29,30</sup> The current hydrogelator was designed based on our experience with strong hydrogelation ability of a phenylalanine derivative (NapF).<sup>10</sup> We surmised that alanine (Ala) can replace Phe in the construction of a molecularly-concise motif capable of undergoing self-assembly. The carboxylic acid end of Ala was converted to hydrazide in order to augment the hydrogen-bonding interactions in the resulting compound.<sup>31,32</sup> The hydrazide unit could also impart chemo-responsive behavior, due to the presence of protonable amine. The molecular structure of the resulting compound, named **Ala-hyd**, is shown in the left panel of Fig. 1. The synthesis and characterization details of **Ala-hyd** are provided in ESI.

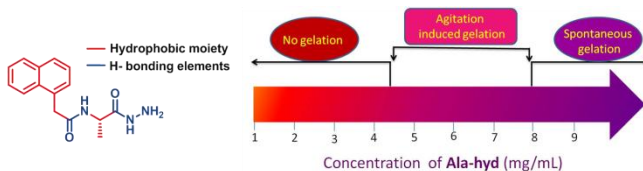


**Fig. 1** Left: Chemical structure of the alanine derivative (**Ala-hyd**). Right: Concentration-dependent hydrogelation profile of **Ala-hyd**.

### 3.2 Apparent $pK_a$ of the amine residue

Acid-base titrimetry was employed to gauge the apparent  $pK_a$  of the amine unit present in **Ala-hyd**.<sup>33</sup> The bi-sigmoidal titration plot for **Ala-hyd** is shown in Fig. S1 of ESI. The first break around pH 7 corresponds to the neutralization of excess acid to form water. A second break, centered at pH 8.9, corresponds to the apparent  $pK_a$  of the protonated amine unit. During the titration, we could observe gradual precipitation of **Ala-hyd** as the pH became >6. At pH ~10, complete phase-separation of a

white solid was seen. These observations indicated that aggregation of **Ala-hyd** starts even in its protonated state. In its unprotonated form (at pH 10), **Ala-hyd** underwent complete phase-separation from the aqueous medium. Results from our lab, and those of others have indicated that compounds with multiple hydrogen bonding sites can undergo significant self-assembly even in their partially charged states.<sup>7,10</sup> In these conditions, the intermolecular electrostatic repulsions are overcome to a certain extent by the hydrogen bonding interactions.

### 3.3 Hydrogelation behavior of Ala-hyd

The compound **Ala-hyd** could be dissolved in aqueous medium (buffered or salt-free) upon heating. Above 8 mg/mL concentration, hydrogels were formed spontaneously when these hot solutions attained room temperature. However, below this concentration, the aqueous solutions of **Ala-hyd** remained stable for a couple of days unless they were mechanically agitated (by stirring, vortexing or sonication). In the concentration range of 4–8 mg/mL (i.e. 0.4–0.8 wt% regime), **Ala-hyd** formed physical hydrogels only when its aqueous solutions were mechanically agitated (see video and Fig. S2, ESI). At concentrations <4 mg/mL, the resulting solutions exhibited significant increase in turbidity upon mechanical agitation (discussed below). However, at these low concentrations, self-supporting gels were not obtained, and only turbid suspensions resulted even after extended mechanical agitation. The overall hydrogelation profile of **Ala-hyd** is summarized in Fig. 1, right panel.

### 3.4 Agitation induced assembly

It is known previously that supersaturated solutions formed by certain short synthetic peptides remain stable unless they are disturbed mechanically.<sup>26</sup> It is likely that something similar is happening with **Ala-hyd** solutions. Our earlier work has shown that molecules containing flexible constituents may require mild agitation (in form of sonication) to induce assembly-formation. Agitation introduces nucleation sites required to initiate the assembly process. In absence of any agitation, this nucleation event may be delayed due to the enhanced structural flexibility present in these molecules, and the supersaturated solution remains stable in absence of the nucleation event happening. The mechano-responsive hydrogelation exhibited by **Ala-hyd** in 4–8 mg/mL concentration range, both in buffered as well as salt-free conditions, was probed further by a variety of techniques, as detailed below.

#### 3.4.1 Turbimetry

Turbidity measurements were performed on the mechanically agitated test sample, as well as on the non-agitated control samples to confirm the agitation-induced aggregation by **Ala-hyd**. As shown in Fig. 2, while turbidity of the vortexed sample increased significantly under these conditions, the non-vortexed sample remained clear. Increase in turbidity of the agitated sample occurred due to the self-assembly of **Ala-hyd**.

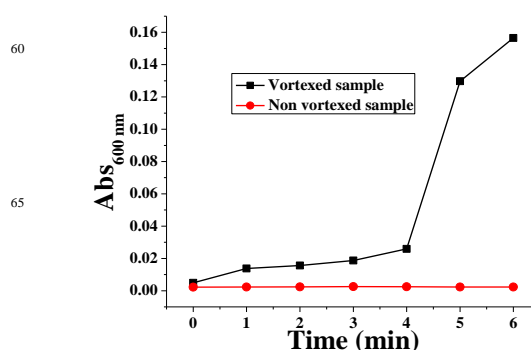


**Fig. 2** Turbidity profiles of **Ala-hyd** samples (1 mg/mL in 50 mM PB pH=7) that were vortexed at 2000 rpm (black) for different time intervals, or were not agitated (red).

#### 3.4.2 Fluorescence spectroscopy

The presence of naphthalene unit in **Ala-hyd**, allowed us to employ fluorescence spectroscopy to probe this agitation-induced self-assembly. At 0.45 mg/mL, aqueous solutions of **Ala-hyd** had fluorescence maximum at 337 nm, and no indication of any excimer formation. Upon vortexing this solution, the fluorescence intensity ( $I_{\text{fl}}$ ) at 337 nm increased considerably (0.45 mg/mL, Fig. 3). However, due to the low concentration of **Ala-hyd**, the sols were almost visually transparent under these conditions. We believe that this increase in  $I_{\text{fl}}$  at 337 is due to formation of assemblies by **Ala-hyd**. In these assemblies, the hydrophobic naphthalene units are shielded from water, resulting in an increase in the  $I_{\text{fl}}$  values. However, the rotational flexibility of the naphthalene units, incorporated as a key design feature of the molecule, prevent their tight stacking in these aggregates; and hence emission due to the naphthalene excimer was not observed even after agitation. Our earlier variable-temperature NMR study on Nap-F had also indicated that  $\pi$ - $\pi$  stacking of the naphthalene units does not occur in those assemblies.<sup>8</sup> This was attributed to the rotational flexibility inherent in the aromatic unit present in Nap-F, as is the case with **Ala-hyd** reported here. It is likely that the aromatic units aid in the formation of proto-assemblies but the final assemblies are stabilized predominantly by intermolecular hydrogen bonding interactions.

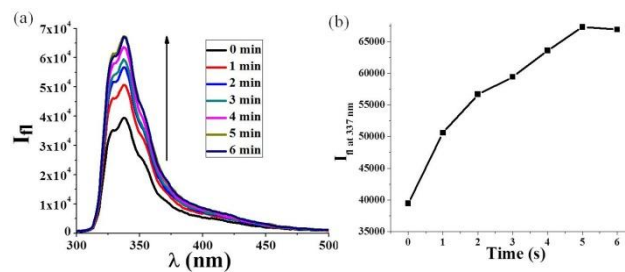


**Fig. 3** (a) Fluorescence spectra recorded at different durations of vortexing of a solution of **Ala-hyd** at 0.45 mg/mL in 50 mM PB (pH=7). (b) Increase in the fluorescence intensity at 337 nm with duration of agitation

#### 3.4.3 FTIR spectroscopy

FTIR spectroscopy experiment was performed to further understand the molecular-level changes that may be causing the

agitation-induced assembly of **Ala-hyd**. For this, **Ala-hyd** solutions in D<sub>2</sub>O were either vortexed at 2000 rpm or left undisturbed. These samples were vacuum-dried and the FTIR spectra recorded (Fig. 4). In the sample dried undisturbed, we observed prominent peaks at 1638 and 1620 cm<sup>-1</sup> for the amide I bands, with a minor hump at 1658 cm<sup>-1</sup>. In polypeptides, these values correspond to  $\beta$ -sheet like conformation. However, vortexing a similar sample resulted in significant changes in its FTIR profile. The band at 1657 cm<sup>-1</sup> became stronger, and a sharpening of all the amide bands was observed. This band position corresponds to  $\alpha$ -helix like conformation in polypeptides. Further, strengthening of the band intensity in the agitated solid sample indicates strengthening of the hydrogen bonds upon agitation.<sup>34</sup> However, any further interpretation of this data may be erroneous. Our efforts to probe the helical content in the assemblies through circular dichroism (CD) were also not successful. We could not obtain discernible CD signatures for these samples either before or after vortexing. This is probably due to the small size of **Ala-hyd** and the presence of single chiral center in it.

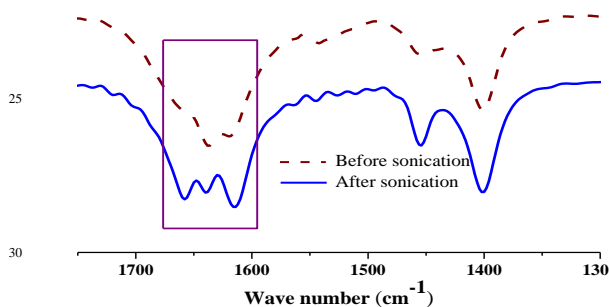


**Fig. 4** FTIR spectra for **Ala-hyd** lyophilized before vortexing (wine) and after vortexing (blue). To minimize solvent interference, the samples were prepared in D<sub>2</sub>O. Rectangular box in the figure highlights the amide I bands that undergo significant changes upon vortexing.

### 3.4.4 Rheological Studies

The self-assembly of **Ala-hyd** had profound influence on the flow behaviour of its aqueous sols. We probed this in detail through rheological studies. The samples were subjected to a unidirectional rotational shearing at constant shear-rates, and the changes in viscosity with time were monitored. We noticed that at all shear rates, after a certain incubation period, there was a rapid increase in the viscosity of the sols, while the buffer on its own did not show any perceptible change in the viscosity under these conditions (Fig. 5a). When the **Ala-hyd** solution was sheared at 2500 rpm, a sharp increase in the viscosity was observed after 400 s. However, a similar sample sheared at the rate of 1500 rpm had an incubation period of 1500 s before an increase in viscosity was seen (Fig. 5b). It is likely that higher shear rates enhance the rate of nucleation of **Ala-hyd** aggregates, resulting in faster aggregation at higher shear rates. The incubation period as well as the maximum viscosity attained was also influenced by the concentration of **Ala-hyd**. Upon increasing the concentration, the incubation period decreased while the maximum viscosity increased. As can be seen in Fig. 5c, increase

in viscosity was observed after 600 s at 7.5 mg/mL concentration; however, decreasing the concentration of **Ala-hyd** to 5 mg/mL increased the incubation period to 1500 s. All the time-dependent rheological experiments revealed the mild shear thickening nature of the **Ala-hyd** aqueous solutions. While these values are not comparable to those obtained for polymeric systems, this result is significant since gels made from low molecular weight compounds are known to exhibit thixotropic behaviour. Further, the concentrations of the gelator used here are significantly lower (at 0.5 wt%) than those employed for studying shear-thickening polymer solutions. Since these gels have >99 wt% water, the bulk shear-viscosity was only marginally higher than that of pure water. However, Fig. S2 (ESI) proves that viscoelastic solids could be obtained upon agitation.

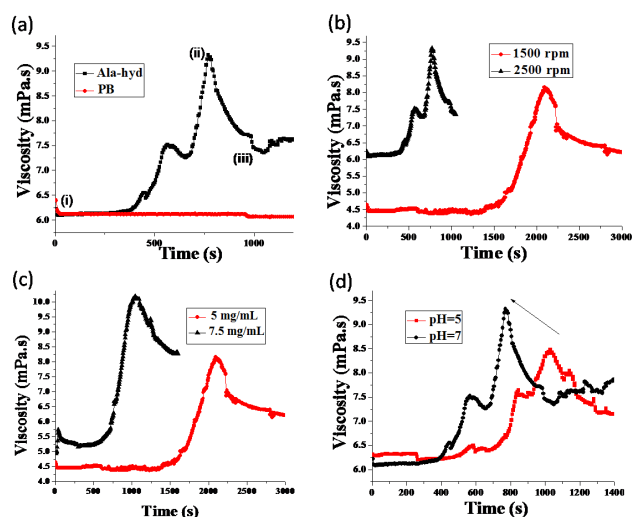


**Fig. 5** (a) Time-dependent changes in the macroscopic viscosity of the sol of **Ala-hyd** (5 mg/mL) upon shearing at 2500 rpm. The markings (i)/(ii)/(iii) in the panel refer to the time points at which samples were extracted for microscopic analysis. (b) Influence of shear rates on the viscosity of the solutions at 5 mg/mL **Ala-hyd**. (c) Effect of **Ala-hyd** concentration on the viscosity of the solutions sheared at 1500 rpm. (d) Influence of pH on the rheological profiles obtained at 2500 rpm, 5 mg/mL **Ala-hyd**.

The presence of hydrazide functionality also imparts chemo-responsive characteristics to **Ala-hyd** in addition to the mechano-responsive nature. Not surprisingly, pH had a strong influence on the self-assembly of this compound. As the pH of the sol of **Ala-hyd** was lowered, it took longer to achieve increase in viscosity upon shearing (Fig. 5d), and the maximum viscosity values were also decreased. This observation is reconciled with weakening of assembly-propensity of **Ala-hyd-H<sup>+</sup>** upon protonation of the amine residue. However, there was a noticeable increase in the viscosity of the solution upon shearing even when the pH of the sol was 2 or 4 units below the pK<sub>a</sub> of **Ala-hyd-H<sup>+</sup>**. This is indicative of strong propensity of **Ala-hyd** to assemble even in its protonated form, due to the presence of multiple hydrogen-bonding sites in this molecule.

We were, however, intrigued by the fluctuations observed in the viscosity profiles shown in Fig. 5a-5c. In all the graphs, the increase in sample viscosity were followed by a decrease as

shearing was continued. These results merited further attention. We also noticed that shearing resulted in the formation of macroscopic fiber like assemblies on the walls of bob/cup (Fig. S3, ESI). We thus undertook detailed microscopic characterizations on the samples extracted at different phases of rheology through scanning electron microscopy (SEM) and atomic force microscopy (AFM).

### 3.4.5 SEM and AFM studies

Microscopic investigations on samples sheared for different durations at 2500 rpm showed the morphological evolution of the assemblies as the sample was sheared. The SEM images shown in Fig. 6a-6c, respectively, correspond to the points (i)-(iii) in Fig. 5a. Initially (i.e. upon shearing for 100 s), only unstructured aggregates were observed (Fig. 6a). However, upon shearing for 800 s, the sample was composed exclusively of an entangled mesh formed by long, high aspect ratio nanofibers (Fig. 6b). This time-point corresponds to highest bulk viscosity exhibited by sols of **Ala-hyd**. In the viscosity decrease phase (point (iii) of Fig. 5a), significant clumping of these fibers could be observed in SEM (Fig. 6c).

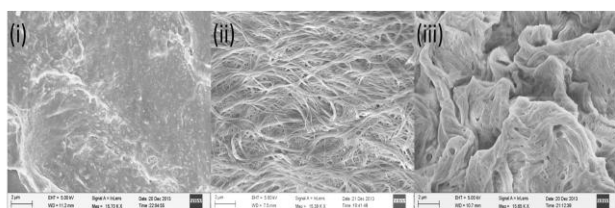


**Fig. 6** Changes in the morphology of assemblies formed by **Ala-hyd** upon shearing at 2500 rpm for different time intervals, as investigated by FE-SEM. Samples were extracted from the bob of rheometer after (i) 100s; (ii) 800 s; and (iii) 1000 s of shearing. These points are marked in the Figure 5a, and correspond to dissimilar macroscopic viscosities.

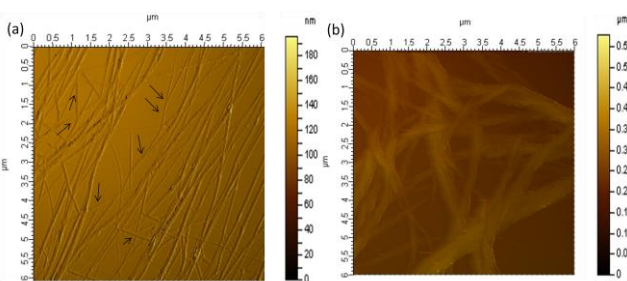


**Fig. 7** (a) AFM image of sample extracted from the bob of rheometer after shearing at 2500 rpm in salt-free water for 800 s. Arrows indicate points where two individual fibers intertwine. (b) The same sample after 1000 s of shearing had much thicker aggregates.

The clumping of fibers results in greater unobstructed flow of the solvent molecules, and hence, the sample exhibits a decrease in viscosity. This shear-induced nanofibrillation was not influenced by the absence of salts. Similar morphological changes were observed in samples sheared in salt-free conditions, as evidenced

by AFM micrograph shown in Fig. 7. In this image inter-twining of the nanofibers could also be observed multiple places. The nanofibrillar assemblies formed upon shearing had a strong right handed helicity, as shown in Fig. 8, reflecting the chirality present in the amino acid.

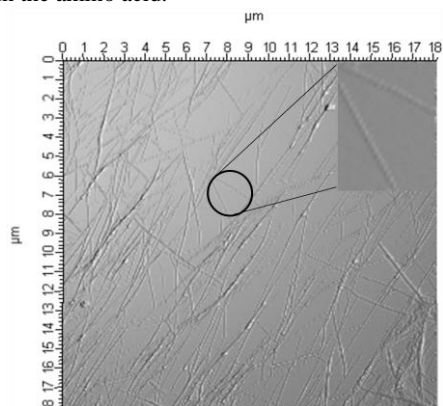


**Fig. 8** AFM image of showing helical nature of the nanofibrillar assemblies formed by **Ala-hyd** upon agitation. Inset shows the presence of right handed helicity in individual nanofibers.

## 4 Conclusions

In conclusion, we have designed a molecularly-concise, low molecular weight hydrogelator derived from alanine. This compound, **Ala-hyd**, has a rotationally-free aromatic *N*-protection, and a hydrazide unit at the carboxylic end of alanine. In medium concentration regime, visually clear aqueous solutions of **Ala-hyd** were stable for a couple of days. Mechanical agitation of these solutions, however, induced rapid self-assembly of **Ala-hyd** into helical nanofibers, and resulted in either increased turbidity or hydrogelation, based on the concentration of **Ala-hyd** present. Due to agitation-induced nanofibrillation of **Ala-hyd**, its aqueous sols were mildly shear-thickening. Time-dependent viscosity measurements showed that the highest viscosity point coincided with the presence of an entangled mesh of self-assembled nanofibers. However, upon continued shearing, these nanofibers clump together, causing lowering of the sample viscosity. The nanofibers had right handed helicity, and inter-twining of fibers could also be observed in AFM. Due to the presence of basic amine residue, **Ala-hyd** was chemo-responsive too, and its self-assembly propensity decreased on decreasing pH.

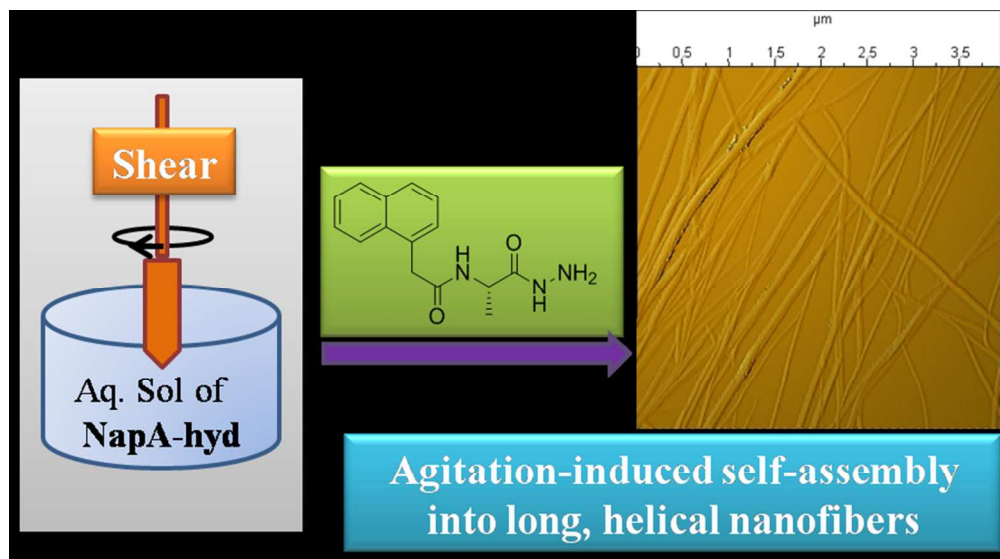
## Acknowledgements

ARM thanks IISER Bhopal for Senior Research Fellowship. AS acknowledges IISER Bhopal for intramural funds and facilities.

## Notes and references

- <sup>a</sup> Department of Chemistry, Indian Institute of Science Education and Research Bhopal, Bhopal – 462 066, India; E-mail: asri@iiserb.ac.in  
<sup>†</sup> Electronic Supplementary Information (ESI) available: [contains synthesis and characterization details, pKa measurement, and rheology studies on **Ala-hyd**]. See DOI: 10.1039/b000000x/  
 L. A. Estroff and A. D. Hamilton, *Chem Rev*, 2004, **104**, 1201–1218.  
 P. Casuso, P. Carrasco, I. Loinaz, H. J. Grande, and I. Odriozola, *Org. Biomol. Chem.*, 2010, **8**, 5455–5458.

3. A. Altunbas, S. J. Lee, S. A. Rajasekaran, J. P. Schneider, and D. J. Pochan, *Biomaterials*, 2011, **32**, 5906–5914.
4. A. R. Hirst, B. Escuder, J. F. Miravet, and D. K. Smith, *Angew. Chem. Int. Ed.*, 2008, **47**, 8002–8018.
5. I. W. Hamley, *Angew. Chem. Int. Ed.*, 2007, **46**, 8128–8147.
6. E. Gazit, *Chem. Soc. Rev.*, 2007, **36**, 1263–1269.
7. E. K. Johnson, D. J. Adams, and P. J. Cameron, *J. Mater. Chem.*, 2011, **21**, 2024–2027.
8. J. J. Panda, A. Mishra, A. Basu, and V. S. Chauhan, *Biomacromolecules*, 2008, **9**, 2244–2250.
9. M.-O. M. Piepenbrock, N. Clarke, J. A. Foster, and J. W. Steed, *Chem. Commun.*, 2011, **47**, 2095–2097.
10. A. Reddy, A. Sharma, and A. Srivastava, *Chem.-Eur. J.*, 2012, **18**, 7575–7581.
11. S. S. Babu, V. K. Praveen, and A. Ajayaghosh, *Chem. Rev.*, 2014, **114**, 1973–2129.
12. X. J. Fu, S. Q. Cao, N. X. Wang, S. Z. Zhang, H. Wang, and Y. J. Yang, *Chin Chem Lett*, 2007, **18**, 1001–1004.
13. L. Meazza, J. A. Foster, K. Fucke, P. Metrangolo, G. Resnati, and J. W. Steed, *Nat. Chem.*, 2013, **5**, 42–47.
14. P. Metrangolo, F. Meyer, T. Pilati, G. Resnati, and G. Terraneo, *Angew. Chem. Int. Ed.*, 2008, **47**, 6114–6127.
15. A. Priimagi, G. Cavallo, P. Metrangolo, and G. Resnati, *Acc. Chem. Res.*, 2013, **46**, 2686–2695.
16. W. Deng and D. H. Thompson, *Soft Matter*, 2010, **6**, 1884–1887.
17. I. Hwang, W. S. Jeon, H.-J. Kim, D. Kim, H. Kim, N. Selvapalam, N. Fujita, S. Shinkai, and K. Kim, *Angew. Chem. Int. Ed.*, 2007, **46**, 210–213.
18. J. P. Schneider, D. J. Pochan, B. Ozbas, K. Rajagopal, L. Pakstis, and J. Kretsinger, *J. Am. Chem. Soc.*, 2002, **124**, 15030–15037.
19. D. Higashi, M. Yoshida, and M. Yamanaka, *Chem.-Asian J.*, 2013, **8**, 2584.
20. H. Hoshizawa, Y. Minemura, K. Yoshikawa, M. Suzuki, and K. Hanabusa, *Langmuir*, 2013, **29**, 14666–14673.
21. K. Liu and J. W. Steed, *Soft Matter*, 2013, **9**, 11699–11705.
22. J. Nanda, A. Biswas, and A. Banerjee, *Soft Matter*, 2013, **9**, 4198–4208.
23. N. C. Crawford, L. B. Popp, K. E. Johns, L. M. Caire, B. N. Peterson, and M. W. Liberatore, *J. Colloid Interfac. Sci.*, 2013, **396**, 83–89.
24. T. Mahmoudi, V. Karimkhani, G. S. Song, D. S. Lee, and F. J. Stadler, *Macromolecules*, 2013, **46**, 4141–4150.
25. S. Ramachandran, Y. Tseng, and Y. B. Yu, *Biomacromolecules*, 2005, **6**, 1316–1321.
26. Z. Xie, A. Zhang, L. Ye, X. Wang, and Z. Feng, *J. Mater. Chem.*, 2009, **19**, 6100–6102.
27. W. Helen, P. de Leonardis, R. V. Ulijn, J. Gough, and N. Tirelli, *Soft Matter*, 2011, **7**, 1732–1740.
28. J. T. van Herpt, M. C. Stuart, W. R. Browne, and B. L. Feringa, *Langmuir*, 2013, **29**, 8763–8767.
29. A. Sharma, Q. Maqbool, and A. Srivastava, *RSC Adv*, 2013, **3**, 18900–18907.
30. P. S. Yavvari and A. Srivastava, *RSC Adv*, 2013, **3**, 17244–17253.
31. C.-S. Wang, X.-H. Wang, Z.-Y. Li, W. Wei, Z.-L. Shi, and Z.-T. Sui, *Bull. Korean Chem. Soc.*, 2011, **32**, 1258–1262.
32. B. O. Okesola and D. K. Smith, *Chem. Commun.*, 2013, **49**, 11164–11166.
33. C. Tang, A. M. Smith, R. F. Collins, R. V. Ulijn, and A. Saiani, *Langmuir*, 2009, **25**, 9447–9453.
34. G. Martinez and G. Millhauser, *J. Struct. Biol.*, 1995, **114**, 23–27.



152x85mm (150 x 150 DPI)